



OPEN

## Prognostic value of pseudotime from texture parameters of FDG PET/CT in locally advanced rectal cancer with neoadjuvant concurrent chemoradiotherapy

Hyunjong Lee<sup>1,5</sup>, Seung Hyup Hyun<sup>1,5</sup>, Yong Beom Cho<sup>2</sup>, Hee Cheol Kim<sup>2</sup>, Hee Chul Park<sup>3</sup>, Young Suk Park<sup>4</sup> & Joon Young Choi<sup>1</sup>✉

Texture analysis generates image parameters from F-18 fluorodeoxyglucose positron emission tomography/computed tomography (FDG PET/CT). Although some parameters correlate with tumor biology and clinical attributes, their types and implications can be complex. To overcome this limitation, pseudotime analysis was applied to texture parameters to estimate changes in individual sample characteristics, and the prognostic significance of the estimated pseudotime of primary tumors was evaluated. Our subjects were 224 rectal cancer patients who underwent pretherapeutic FDG PET/CT and neoadjuvant concurrent chemoradiation therapy (CCRT). Texture parameters of the primary tumor were extracted from FDG PET/CT images acquired before neoadjuvant CCRT. The pseudotime of the primary tumor was successfully derived from texture parameters using the Phenopath tool. Clinico-pathologic features were obtained and survival analysis was performed. Pseudotime, metabolic tumor volume (MTV), and total lesion glycolysis (TLG) demonstrated significant associations with overall survival. Unlike MTV and TLG, pseudotime was an independent prognostic factor for overall survival (hazard ratio = 4.807, p-value = 0.037). Pseudotime analysis integrates various metabolic texture parameters into a single metric. Pseudotime estimated from FDG PET/CT images of primary tumors shows superior prognostic significance to conventional PET parameters in patients with locally advanced rectal cancer treated with tri-modality therapy.

**Keywords** Rectal cancer, FDG PET/CT, Texture analysis, Prognosis, Pseudotime analysis

F-18 fluorodeoxyglucose positron emission tomography/computed tomography (FDG PET/CT) is an effective imaging technique for diagnosing and guiding the treatment of rectal cancer<sup>1,2</sup>. The maximum standardized uptake value (SUVmax) is a strong prognostic indicator for both disease-free survival (DFS) and overall survival (OS) in rectal cancer<sup>3,4</sup>. In addition, volumetric parameters such as metabolic tumor volume (MTV) and total lesion glycolysis (TLG) have shown significant prognostic value in patients with rectal cancer undergoing various treatment options<sup>5,6</sup>.

Radiomics, an emerging field in radiology and nuclear medicine, involves extracting texture features from medical images using various algorithms<sup>7</sup>. These texture parameters, beyond conventional metabolic and volumetric parameters, are hypothesized to be linked to tumor biology and prognosis in rectal cancer patients. For instance, several parameters, such as contrast, homogeneity, and coefficient of variation, have been identified as significant prognostic factors for survival or disease progression in rectal cancer<sup>8,9</sup>. Despite previous studies demonstrating the clinical significance of texture parameters, extracting consistently reliable parameters that

<sup>1</sup>Department of Nuclear Medicine, Samsung Medical Center, Sungkyunkwan University School of Medicine, 81 Irwon-Ro, Gangnam-Gu, Seoul 06351, Republic of Korea. <sup>2</sup>Department of Surgery, Samsung Medical Center, Sungkyunkwan University School of Medicine, Seoul, Republic of Korea. <sup>3</sup>Department of Radiation Oncology, Samsung Medical Center, Sungkyunkwan University School of Medicine, Seoul, Republic of Korea. <sup>4</sup>Division of Hematology-Oncology, Department of Medicine, Samsung Medical Center, Sungkyunkwan University School of Medicine, Seoul, Republic of Korea. <sup>5</sup>Hyunjong Lee and Seung Hyup Hyun contributed equally to this work. ✉email: jynm.choi@samsung.com

reflect the aggressiveness of the tumor or prognosis is often difficult. Moreover, the clinical implications or meanings of each texture parameter can be hard to interpret due to the complex and intricate nature of the algorithms. To overcome this limitation, a previous study attempted to integrate multiple parameters to produce a single indicator: pseudotime<sup>10</sup>.

Pseudotime analysis is a prominent method used to investigate changes in cell or tissue characteristics based on transcriptomic data<sup>11</sup>. It assigns a numerical value indicating the progression stage or evolution state of a cell or tissue in the disease course. Previous research has applied pseudotime analysis to study cellular dynamics in rectal cancer<sup>12,13</sup>. RNA-sequencing data and radiomics data share the common characteristic of being high-dimensional and complex, making pseudotime analysis applicable to radiomics data. From this perspective, a previous study attempted to apply pseudotime analysis to FDG PET/CT images of lung cancer<sup>10</sup>. However, the notable lack of research in this area underscores the need for additional evidence to support the utility of pseudotime analysis in radiomics.

Herein, metabolic texture parameters were extracted from FDG PET/CT images from patients with rectal cancer. Pseudotime analysis was performed on the texture parameters of the primary tumor. The prognostic significance of the pseudotime parameter of primary tumors was compared with that of conventional metabolic and volumetric parameters of FDG PET/CT in patients with locally advanced rectal cancer who have undergone neoadjuvant concurrent chemoradiotherapy (CCRT).

## Methods

### Subjects

This study retrospectively enrolled 239 patients undergoing FDG PET/CT scans for the initial staging of rectal cancer before neoadjuvant CCRT between January 2008 and December 2016. Two patients were excluded due to the absence of initial or post-CCRT carcinoembryonic antigen (CEA) results. Six patients who underwent a non-total mesorectal excision technique were excluded due to the absence of pathological results after neoadjuvant CCRT. Four patients were excluded due to the absence of histological grade data. Three patients with metabolic tumor volumes smaller than 5 cm<sup>3</sup> were excluded based on previous studies suggesting that the minimum MTV eligible for radiomics analysis in FDG PET/CT is approximately 5 cm<sup>3</sup><sup>14,15</sup>. Finally, 224 patients who underwent tri-modality therapy were included in this study (Fig. 1). Samsung Medical Center Institutional Review Board approved this retrospective cohort study (#2024-06-070). Informed consent was waived by Samsung Medical Center Institutional Review Board. All methods were performed in accordance with the Declaration of Helsinki.

Neoadjuvant CCRT was decided through a multidisciplinary team approach and performed as described in a previous study<sup>6</sup>. In brief, radiation was administered to the whole pelvic field at a total dose of 50.4 Gy in 25 fractions. Chemotherapy was administered concurrently with radiation based on 5-fluorouracil (5-FU) or capecitabine. 5-FU (425 mg/m<sup>2</sup>/day) and leucovorin (20 mg/m<sup>2</sup>/day) were administered intravenously for 5 days during the first and fifth weeks of radiotherapy. Oral capecitabine (825 mg/m<sup>2</sup>/day) was administered twice daily during the period of radiotherapy. All patients underwent curative resection with an 8-week interval from the completion of CCRT.

### FDG PET/CT acquisition

All patients fasted for at least six hours and had blood glucose levels of less than 200 mg/dL at the time of their FDG PET/CT scans. Whole-body PET and CT images from basal skull to mid-thigh were acquired 60 min after an injection of 5.0 MBq/kg FDG without intravenous or oral contrast on a Discovery LS or a Discovery STE PET/CT scanner (GE Healthcare, Milwaukee, WI, USA). Continuous spiral CT was performed with an 8-slice helical CT (140 keV, 40–120 mA; Discovery LS) or 16-slice helical CT (140 keV, 30–170 mA; Discovery STE). An emission scan was then obtained from head to thigh for 4 min per frame in 2-dimensional mode (Discovery LS) or 2.5 min per frame in 3-dimensional mode (Discovery STE). PET images were reconstructed using CT for attenuation correction by the ordered-subset expectation maximization algorithm with 28 subsets and 2 iterations (matrix 128 × 128, voxel size 4.3 × 4.3 × 3.9 mm; Discovery LS) or ordered-subset expectation maximization algorithm with 20 subsets and 2 iterations (matrix 128 × 128, voxel size 3.9 × 3.9 × 3.3 mm; Discovery STE). SUV was calculated by adjusting for the administered FDG dose and the patient's body weight.

### FDG PET/CT image analysis

Image feature extraction was performed using a threshold segmentation method with an SUV threshold of 2.5, applied through MIM software version 6.4 (MIM Software Inc., Cleveland, OH, USA). Briefly, an experienced nuclear medicine physician, blinded to all clinical data except for the target tumor location, identified the primary tumor. Starting from the tumor's center, the physician extended the cursor toward the lesion boundary, allowing the software to automatically generate a three-dimensional volume of interest encompassing areas with an SUV above 2.5. Following segmentation of the primary tumor lesion, PET image features were extracted using the Chang-Gung Image Texture Analysis (CGITA) toolbox, an open-source software implemented in MATLAB (version 2012a; MathWorks Inc., Natick, MA, USA)<sup>16</sup>. This analysis measured 86 texture features available in CGITA for each segmented area, including conventional metrics such as SUVmax, SUVmean, MTV, and TLG. Among total 86 parameters, redundant or duplicated parameters were excluded. Finally, an input dataset consisted of 56 radiomic parameters including texture parameters from voxel alignment matrix, neighborhood intensity difference, intensity size zone matrix, normalized cooccurrence matrix, and neighboring gray level dependence.

### Pseudotime estimation

Pseudotime analysis was performed by the same methodology described in the previous study<sup>10</sup>. In brief, a pseudotime trajectory was generated using the "Phenopath" package in R<sup>13</sup>. For preprocessing, ComBat

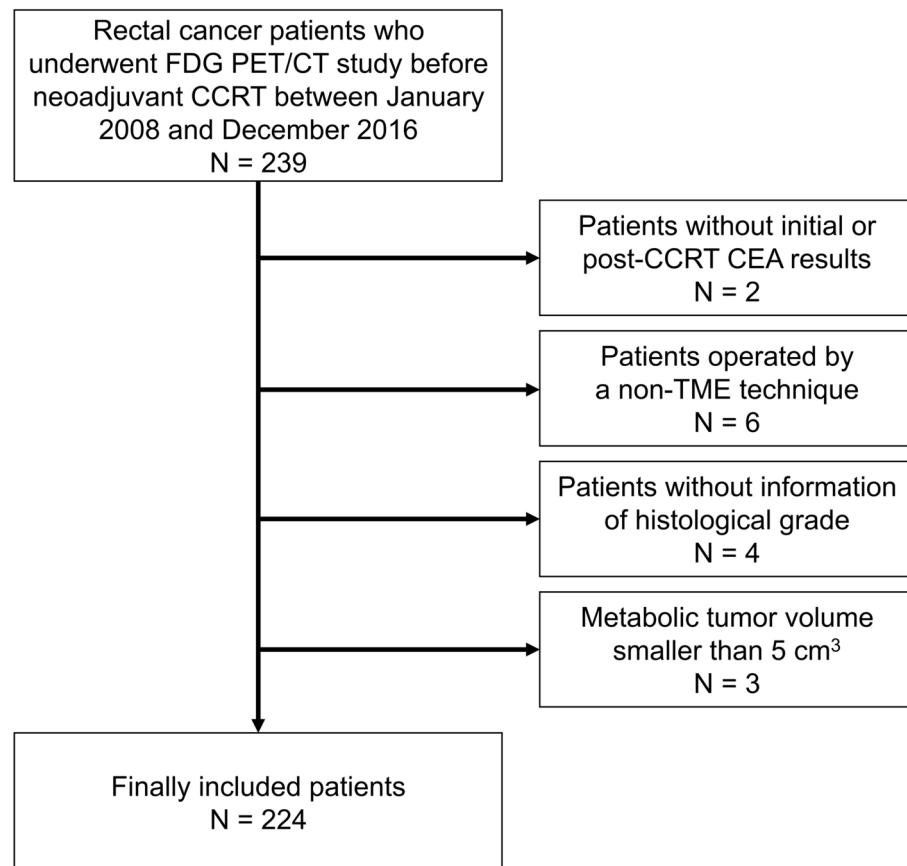


**Fig. 1.** Patient inclusion and exclusion criteria. Initially, 239 consecutive patients were retrospectively enrolled. Among them, two patients without initial or post-CCRT CEA results were excluded. Six patients operated by a non-total mesorectal excision technique were excluded. Four patients without histological grade data were excluded. Three patients with metabolic tumor volumes smaller than  $5\text{ cm}^3$  were excluded. Ultimately, 224 patients were included.

harmonization was conducted to remove batch effects due to various PET/CT instruments using the package “neuroCombat” in R. Subsequently, corrected texture parameters were normalized using the “scale” function in R. The input data were a normalized texture parameter matrix of initial FDG PET/CT images. We chose an evidence lower bound (ELBO) of  $10^{-6}$  computed thinned by 2 iterations. Then, the Phenopath algorithm repeated calculations to predict pseudotime with 2 iterations until ELBO reached below  $10^{-6}$ . ELBO is a quantity that reflects optimized approximation in probabilistic inference<sup>17</sup>. The Phenopath algorithm models texture parameters in terms of a pseudotime using Bayesian statistics, which assigns a probabilistic progression stage to each subject. Ultimately, pseudotime was estimated as a reference value for the latent progression of texture characteristics from FDG PET/CT. Pseudotime was normalized with a range of 0 to 1 for further analysis.

### Clinical variables and follow-up

Clinical information including sex, age, performance of adjuvant therapy, and histological grade of the primary tumor was obtained by reviewing electronic medical records. Evaluation of the clinical tumor stage (cT stage) was based on the invasion of the primary tumor as determined by MRI or CT scans. The clinical nodal stage (cN stage) was evaluated by the maximal number of lymph nodes positive for metastasis in MRI, CT, or FDG PET/CT scans. After we reviewed the pathologic reports of surgical specimens, pathological T (pT) and N (pN) stages were determined. The determination of all the clinical and pathological stages was based on the AJCC/UICC staging system, eighth edition. Pathological complete remission (pCR) was defined as no tumor and lymph node metastasis after neoadjuvant CCRT.

Adjuvant therapy was performed after surgery according to the situation of each patient and the corresponding decision of their physician. After surgery, all patients were monitored regularly to obtain accurate information regarding recurrence. The follow-up program was every 2–4 months during the first year, every 4–6 months during the next 2 years, and every year thereafter. Every follow-up evaluation included a complete physical examination, complete blood count, and biochemical screening including CEA. CT scans of the abdomen and pelvis were performed from every 6 months to 1 year, or more frequently if clinically indicated.

Recurrence or metastasis was considered when there was an abnormal finding suggesting recurrence or metastasis on serial imaging studies or pathologically confirmed malignancy. The events for survival analysis

were defined as recurrence or metastasis and any cause of death. The disease-free and OS durations from the last follow-up or event were recorded for each patient.

### Statistical analysis

Correlation analyses were performed to reveal associations between image parameters and estimated pseudotime. Pearson's correlation analysis was performed for each image parameter and pseudotime. Age and CEA were recorded as a continuous scale and divided into two groups as discrete scales according to a cutoff value to best discriminate the prognosis of OS in all patients. They were explored by the "surv\_cutpoint" function in package "survminer". The clinical variables used for survival analysis included sex, age by both discrete and continuous scales, location of the primary tumor, cT stage, clinical TNM stage, performance of adjuvant therapy, CEA by both discrete and continuous scales, histological grade of primary tumor, treatment response, pT stage, and pathological TNM stage. For FDG PET/CT images, SUVmax, SUVmean, MTV, TLG, and pseudotime were selected as variables. These five parameters were recorded as continuous scales and divided into two groups as discrete scales according to a cutoff value to best discriminate the prognosis of OS in all patients by the "surv\_cutpoint" function. SUVmax, SUVmean, MTV, TLG, and pseudotime were used with both discrete and continuous scales for survival analysis.

OS and DFS were the endpoints of the analysis. The Cox proportional hazards model was used to evaluate the prognostic power of each variable. Hazard ratios (HRs) and 95% confidence intervals were estimated. Log-rank statistics were also obtained by the Kaplan-Meier method. Significant variables in univariate survival analysis with p-values of log-rank statistics lower than 0.05 were included in multivariate survival analysis. Variables with collinearity were excluded. Due to multicollinearity issues, multivariate survival analysis was performed repeatedly according to each image parameter. All statistical analyses were performed using R software (v.4.1.2, R Foundation for Statistical Computing, Vienna, Austria). A p-value lower than 0.05 was considered statistically significant.

## Results

### Demographic data

The clinical characteristics and demographics of the subjects are described in Table 1. Overall, 65.6% of the patients were male, with a median age of 57.5 years. Adjuvant chemotherapy was administered to 86.5% of the subjects. Regarding clinical stages, 60.7% of the subjects were classified as stage IIIB. Among histological grades, moderately differentiated tumors were the most common, accounting for 65.2% of cases. Residual primary tumors were not found after an operation in 14.7% of cases (ypT0), and pCR was achieved in 12.9% of the subjects.

### Pseudotime estimation

The pseudotime of the primary tumor was effectively calculated in the texture parameter datasets. A principal component analysis plot was used to illustrate the sequence of pseudotime in each FDG PET/CT image (Fig. 2A) and showed that pseudotime was determined in a specific direction rather than randomly. A total of 31 parameters showed positive correlations with pseudotime, and 25 parameters showed negative correlations with pseudotime. The top 10 features are displayed in Fig. 2B and detailed statistics for all parameters are described in Supplementary Table 1. Homogeneity, second moment, inverse difference moment, intensity variability, and dissimilarity showed positive correlations with pseudotime. Cooccurrence entropy, neighboring gray level dependence entropy, coarseness, complexity, and short-run emphasis showed negative correlations with pseudotime. In addition, correlation analysis was performed between conventional image parameters and pseudotime. SUVmax, SUVmean, MTV, and TLG all showed positive correlations with pseudotime (Fig. 3,  $r=0.478$ ,  $r=0.529$ ,  $r=0.981$ ,  $r=0.899$ , respectively;  $p < 0.001$  for all).

### Survival analysis

In univariate survival analysis, initial CEA, post-CCRT CEA with continuous scale, and pathological N stage after CCRT (ypN) were significant prognostic factors for DFS (Table 2). None of the conventional parameters from FDG PET/CT images were significant prognostic factors for DFS. Although pseudotime with a discrete scale showed a lower p-value than conventional image parameters, it was not statistically significant (Table 2).

Age with continuous scale, age with discrete scale, adjuvant chemotherapy, clinical T stage, initial CEA, post-CCRT CEA with continuous scale, pathological T stage after CCRT (ypT), ypN, MTV with discrete scale, TLG with discrete scale, and pseudotime with discrete scale were significant prognostic factors for OS (Table 2). In the multivariate survival analysis, pseudotime was selected as an independent prognostic factor for OS (Table 3). In contrast, MTV and TLG were not independent prognostic factors for OS. MTV with discrete scale, TLG with discrete scale, and pseudotime with discrete scale effectively discriminated the risk of OS (Fig. 4).

## Discussion

In this study, pseudotime analysis for primary tumors was successfully implemented on radiomics data obtained from FDG PET/CT images in patients with rectal cancer treated by tri-modality therapy for the first time. Several texture parameters were found to have significant correlations with estimated pseudotime. Pseudotime was a significant prognostic factor in univariate survival analysis for OS. Notably, it was an independent prognostic factor in multivariate analysis for OS, unlike MTV and TLG.

Radiomics involves the extraction of image features from medical images using mathematical algorithms, resulting in the calculation of various texture parameters. Previous research has demonstrated the prognostic value of texture parameters in rectal cancer. For instance, Lovinfosse et al. demonstrated that homogeneity and

Characteristics	Patients, n (%)
Sex	
Female	77 (34.4)
Male	147 (65.6)
Age, median (range), years	57.5 (27–83)
< 66	177 (79.0)
66 ≤	47 (21.0)
Adjuvant chemotherapy	
No	29 (12.9)
Yes	195 (87.1)
Clinical T stage	
T2	17 (7.6)
T3	192 (85.7)
T4	15 (6.7)
Clinical N stage	
N1	87 (38.8)
N2	137 (61.2)
Clinical TNM stage	
IIA	9 (4.0)
IIIA	10 (4.5)
IIIB	136 (60.7)
IIIC	69 (30.8)
Initial CEA, median (range), ng/ml	2.5 (0.5–174.8)
< 5.5	169 (75.4)
5.5 ≤	55 (24.6)
Post-CCRT CEA, median (range), ng/ml	1.4 (0.5–25.1)
< 0.8	50 (22.3)
0.8 ≤	174 (77.7)
Histological grade	
Well-differentiated	72 (32.1)
Moderately differentiated	146 (65.2)
Poorly differentiated	6 (2.7)
Pathological T stage after CCRT	
ypT0	33 (14.7)
ypTis/T1	12 (5.4)
ypT2	69 (30.8)
ypT3	102 (45.5)
ypT4	8 (3.6)
Pathological N stage after CCRT	
ypN0	167 (74.6)
ypN1	43 (19.2)
ypN2	14 (6.2)
Pathological CR	
Yes	29 (12.9)
No	195 (87.1)
SUVmax, median (range)	13.1 (4.0–42.8)
< 10.0	44 (19.6)
10.0 ≤	180 (80.4)
SUVmean, median (range)	4.7 (2.5–12.5)
< 5.8	173 (77.2)
5.8 ≤	51 (22.8)
MTV, median (range), cm <sup>3</sup>	30.6 (6.5–146.2)
< 22.6	67 (29.9)
22.6 ≤	157 (70.1)
TLG, median (range)	140.0 (22.5–1705.4)
< 88.1	54 (24.1)
88.1 ≤	170 (75.9)
Continued	

Characteristics	Patients, n (%)
Pseudotime, median (range)	0.25 (0–1)
<0.16	57 (25.4)
0.16≤	167 (74.6)
Instrument	
Discovery LS	60 (26.8)
Discovery STE	164 (73.2)

**Table 1.** Demographic and clinical characteristics of patients with rectal cancer.

coarseness from FDG PET/CT images in locally advanced rectal cancer were significantly associated with DFS<sup>8</sup>. Bundschuh et al. revealed that heterogeneity assessed by the coefficient of variation from FDG PET/CT images was superior to the conventional parameters to predict the prognosis of rectal cancer patients<sup>9</sup>. Despite these findings, the clinical application of radiomics faces challenges due to the complex and less easily understood biological implications of texture parameters, which are mathematical constructs. Furthermore, there is no consensus on the most appropriate texture parameter among nuclear medicine physicians, underscoring the need for an integrated parameter derived from multiple texture parameters.

Pseudotime analysis is an emerging method used to estimate the genetic or biological evolution of cells or tissues based on large-scale transcriptomic expression data<sup>11</sup>. This method integrates data from multiple cross-sectional specimens into a continuous dataset reflecting temporal evolution. The methodology of pseudotime analysis encompasses over 70 distinct approaches, each with unique characteristics and algorithms. Methods such as Monocle and Slingshot, widely used in single-cell RNA transcriptomic data, involve dimension reduction, clustering, and trajectory estimation. Phenopath, chosen for this study, uses Bayesian statistics to integrate linear regression, estimating the ordering of high-dimensional data across individuals. Phenopath has previously demonstrated its utility in analyzing tissue RNA-seq data from rectal cancer, illustrating its effectiveness<sup>13</sup>. Additionally, it has been successfully applied to FDG PET/CT texture parameters in other cancer types such as lung cancer, validating its prognostic utility<sup>10</sup>. Given its reliance on linear regression modeling, Phenopath is assumed to provide a rational methodology reflecting the disease progression stage clinically. Therefore, Phenopath was used in this study for pseudotime analysis.

Our findings indicate strong associations between pseudotime and conventional PET parameters such as SUVmax, SUVmean, MTV, and TLG, which typically increase with the progression of cancer. Consequently, estimated pseudotime emerged as a significant indicator of disease progression in rectal cancer. The clinical advantages of pseudotime include its ability to stratify high-risk patients for OS and its potential as a more significant prognostic factor than conventional volumetric parameters. A previous study has suggested that tumor heterogeneity might be more closely linked to treatment response and survival than conventional parameters, supporting the utility of pseudotime derived from texture parameters, especially in patients with locally advanced rectal cancer<sup>9</sup>. Therefore, the prognostic value of the new metric created by integrating texture parameters aligns with existing research while also suggesting a novel, clinically applicable prognostic indicator.

In addition to the above, various texture parameters showed significant correlations with estimated pseudotime. For instance, homogeneity, intensity variability, and dissimilarity demonstrated positive correlations with pseudotime, while cooccurrence entropy, neighboring gray level dependence entropy, and complexity showed negative correlations with pseudotime. The negative correlation between entropy-related parameters and pseudotime suggests that as the disease progresses, tumor heterogeneity decreases, reflecting less disorder and complexity in the tumor texture. On the other hand, the positive correlation between homogeneity and pseudotime suggests that as tumors progress, the uniformity within the tumor increases. However, variability and dissimilarity also showed similar trends to homogeneity. This dual pattern suggests that while overall homogeneity increases with tumor progression, there are also increasing regions of local variability as the overall tumor volume grows. Nonetheless, understanding the relationship between the biological heterogeneity of the tumor and the heterogeneity observed in imaging requires further investigation.

To enhance the clinical utility of pseudotime analysis, two additional conditions should be considered. First, it is better to accurately predict responses to neoadjuvant CCRT, not just survival. If it proves to be a good predictor of pCR, its prognostic value would be significantly enhanced. In this study, an attempt was made to predict pCR. Pseudotime showed a significant correlation with pCR in univariate logistic regression analysis (data not shown,  $p = 0.047$ ), whereas existing PET parameters on a continuous scale did not. However, pseudotime did not remain a significant independent factor in the multivariate analysis. In contrast, MTV on a discrete scale emerged as an independent significant factor. Therefore, the superiority of pseudotime in predicting pCR cannot be concluded. Second, external validation is required. An attempt was made to collect and analyze data from patients at other institutions, but due to a small sample size and exclusion of subjects, significant results could not be obtained.

In this study, the prognostic significance of PET parameters was evident primarily when analyzed as discrete rather than continuous variables. This may be due to non-linear relationships between these parameters and survival outcomes or to limitations in sample size that restricted our ability to detect linear trends. Subtle prognostic differences could have been diluted, reducing statistical power. Discretizing the parameters into clinically relevant groups enhanced their ability to reveal prognostic differences and allowed for more effective patient stratification. This approach aligns with clinical practice, where threshold values often provide more actionable guidance in risk assessment.

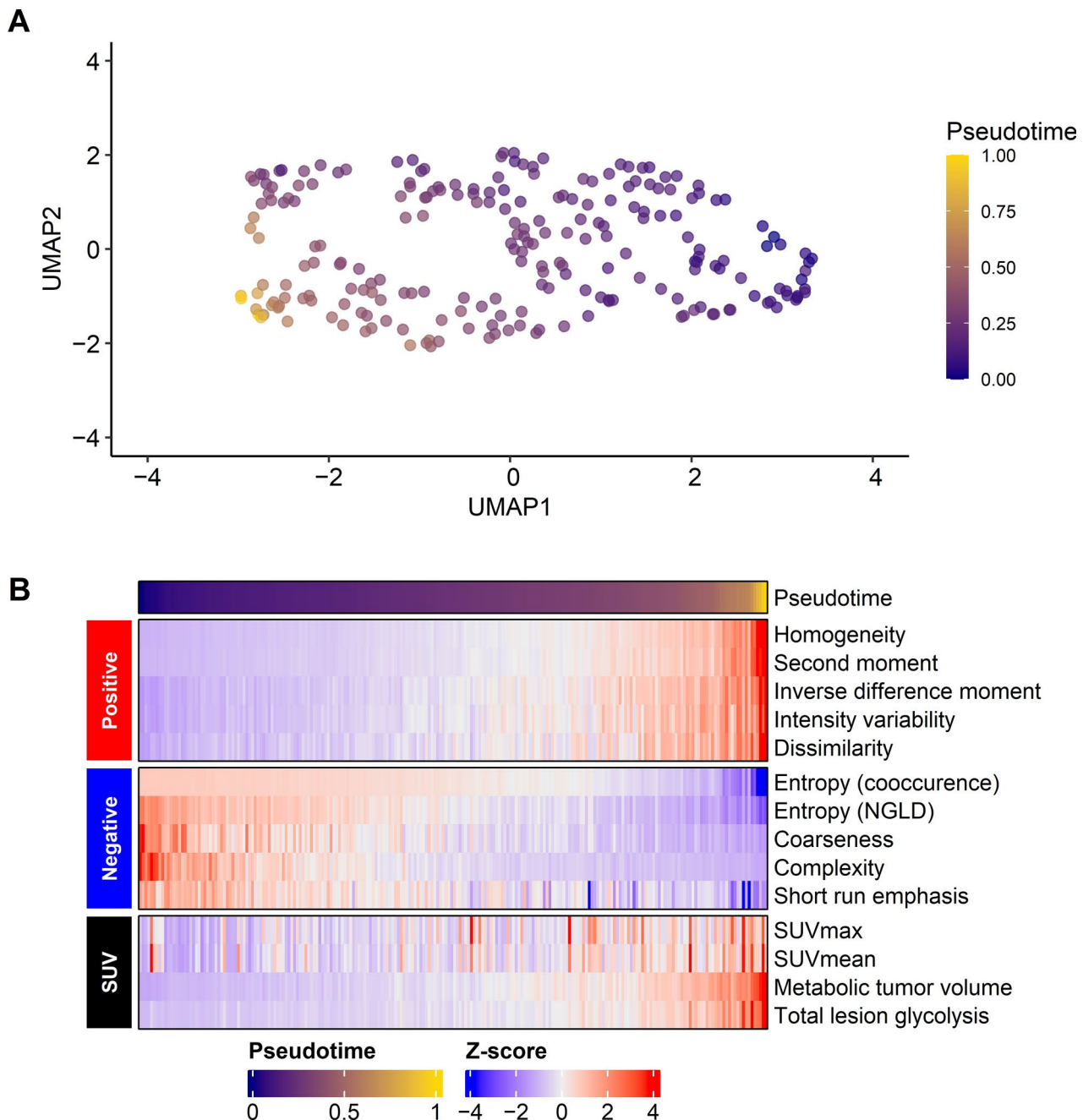


**Fig. 2.** Pseudotime analysis results. The pseudotime of primary tumors was effectively derived from radiomics data. (A) A principal component analysis plot illustrated the sequential order of pseudotime for each FDG PET/CT image. Although no distinct clustering was observed, the estimation of pseudotime followed a particular direction rather than being random. (B) The top 10 features showing positive correlations and the top 10 features showing negative correlations with pseudotime are demonstrated. Additionally, conventional image parameters based on the SUV are included.

This study has several limitations. Firstly, it included only subjects undergoing neoadjuvant CCRT as the initial treatment, which may limit the generalizability of the findings. Previous studies in lung cancer have shown that pseudotime has significant prognostic value in patients who received neoadjuvant CCRT, justifying the selection of this patient group. Additionally, patients with advanced stages tend to have a sufficiently large MTV, allowing for meaningful extraction of texture parameters. Therefore, we focused on patients with locally advanced rectal cancer. A larger cohort including patients with other treatment options is being collected for future studies. Secondly, the study was conducted on a relatively small number of patients from a single institution retrospectively. Additionally, optimal cutoff values to achieve better stratification of prognosis may raise a concern of potential overfitting, which necessitates validation. We attempted validation using data from another institution. However, we were unable to obtain statistically significant results due to the limited sample

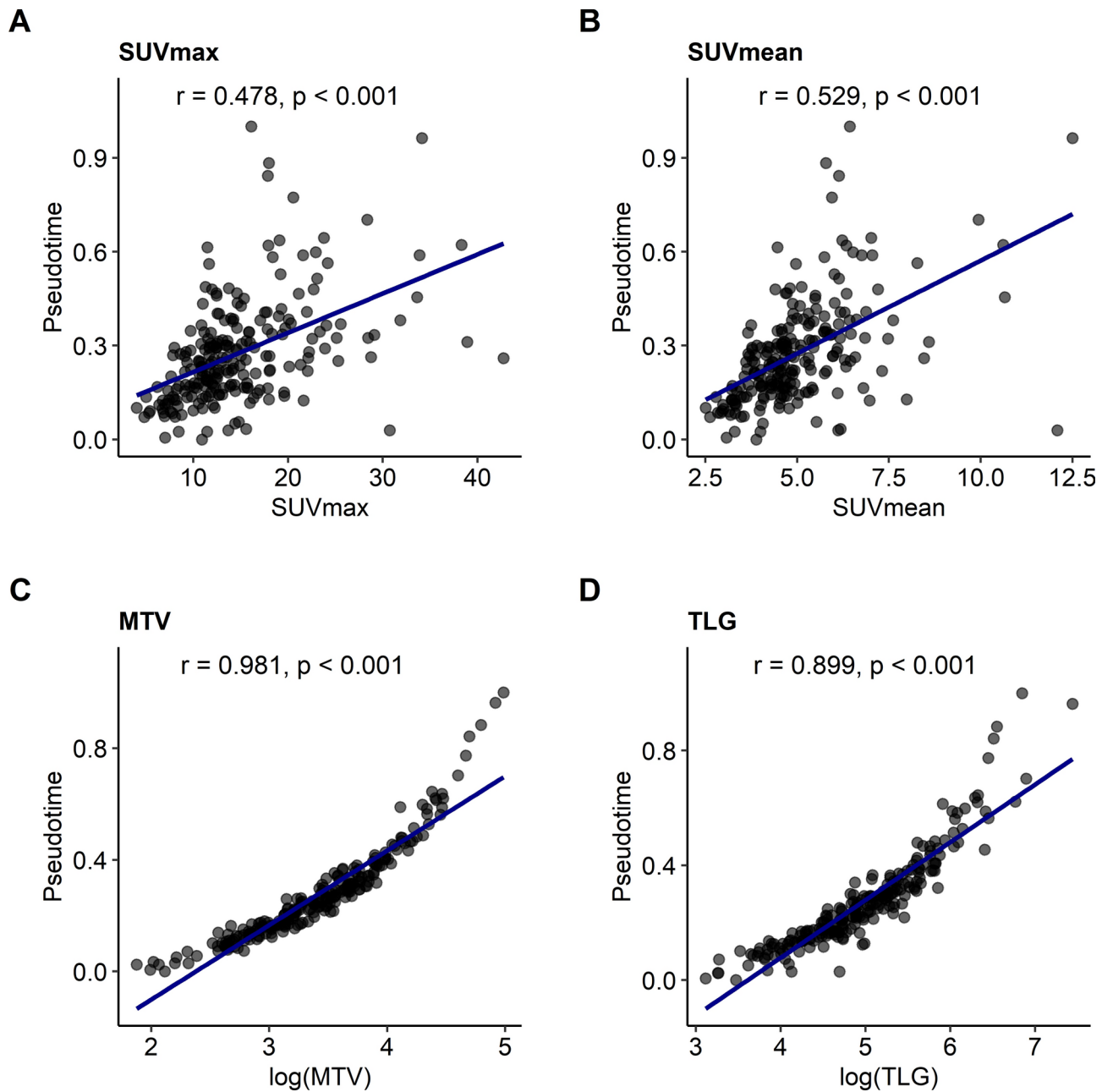


**Fig. 3.** Correlation analysis between image parameters and pseudotime. (A,B) Pseudotime showed a moderate positive correlation with both SUVmax and SUVmean. (C,D) Strong positive correlations were observed between MTV, TLG, and pseudotime.

size of 67 patients. Further investigation for the prognostic value of pseudotime through multicenter prospective studies with larger cohorts is needed. Thirdly, this study only used the texture parameters from FDG PET/CT to calculate pseudotime. Since MRI is widely used for the diagnosis and staging of rectal cancer, various metrics from MRI images such as the ADC map could also be considered for the calculation of pseudotime. This offers a more comprehensive understanding of tumor heterogeneity and may improve the robustness of pseudotime analysis.

To summarize, pseudotime was effectively derived from texture parameters of primary tumors in FDG PET/CT images of locally advanced rectal cancer who underwent neoadjuvant CCRT. Pseudotime demonstrated a good stratification power for prognosis and was an independent prognostic factor for OS unlike conventional volumetric parameters. Pseudotime analysis demonstrates potential as a valuable tool in the clinical assessment and prognosis of rectal cancer patients.

Variable	Categories	Disease-free survival				Overall survival			
		HR	95% CI	P	P of LRT	HR	95% CI	P	P of LRT
Sex	Female vs. male	0.627	0.367–1.073	0.088	0.085	0.811	0.412–1.595	0.543	0.542
Age	< 66 vs. 66 ≤	0.961	0.483–1.910	0.909	0.994	3.224	1.631–6.372	< 0.001	0.002
Age (1-yr increase)		1	0.976–1.025	1		1.059	1.024–1.095	< 0.001	
Adjuvant chemotherapy	No vs. yes	0.702	0.331–1.487	0.352	0.35	0.250	0.122–0.513	< 0.001	< 0.001
Clinical T stage	T2 vs. T3	2.214	0.537–9.120	0.271	0.244	0.905	0.271–3.022	0.871	0.007
	T2 vs. T4	3.789	0.734–19.580	0.112		3.404	0.833–13.907	0.088	
Clinical N stage	N1 vs. N2	1.002	0.580–1.732	1	0.994	0.978	0.496–1.925	0.948	0.948
Clinical stage	IIA/IIIA vs. IIIB	1.277	0.453–3.604	0.644	0.851	2.132	0.491–9.267	0.312	0.421
	IIA/IIIA vs. IIIC	1.129	0.376–3.384	0.829		1.465	0.310–6.923	0.630	
Initial CEA	Low vs. high	2.154	1.240–3.744	0.006	0.005	2.811	1.426–5.540	0.003	0.002
Initial CEA (continuous)		1.005	0.991–1.018	0.516		1.007	0.993–1.022	0.318	
Post-CCRT CEA	Low vs. high	2.526	1.081–5.903	0.032	0.027	5.134	1.231–21.410	0.025	0.012
Post-CCRT CEA (continuous)		1.126	1.042–1.217	0.003		1.107	1.037–1.183	0.002	< 0.001
Histological Grade	WD vs. MD	0.710	0.408–1.236	0.226	0.351	1.111	0.540–2.285	0.775	0.944
	WD vs. PD	1.420	0.332–6.066	0.636		1.297	0.167–10.087	0.804	
Pathological T stage after CCRT	ypT0 vs. ypT1/is	0.513	0.060–4.393	0.543	0.009	0.700	0.078–6.281	0.750	0.041
	ypT0 vs. ypT2	1.043	0.362–3.003	0.938		0.687	0.193–2.441	0.561	
	ypT0 vs. ypT3	2.612	1.021–6.681	0.045		1.889	0.648–5.511	0.244	
	ypT0 vs. ypT4	3.417	0.816–14.303	0.093		4.046	0.900–18.187	0.068	
Pathological N stage after CCRT	ypN0 vs. ypN1	2.597	1.413–4.774	0.002	< 0.001	4.708	2.240–9.896	< 0.001	< 0.001
	ypN0 vs. ypN2	4.083	1.871–8.914	< 0.001		6.942	2.787–17.288	< 0.001	
Pathological CR	No vs. yes	0.468	0.169–1.295	0.144	0.134	0.389	0.093–1.619	0.194	0.178
SUVmax	Low vs. high	1.587	0.748–3.367	0.229	0.225	2.256	0.795–6.400	0.126	0.116
SUVmax (continuous)		1.023	0.985–1.063	0.238		1.027	0.981–1.076	0.255	
SUVmean	Low vs. high	1.152	0.627–2.118	0.648	0.648	1.772	0.881–3.566	0.109	0.104
SUVmean (continuous)		1.032	0.875–1.218	0.706		1.022	0.827–1.263	0.842	
MTV	Low vs. high	1.423	0.762–2.656	0.268	0.266	3.527	1.244–9.998	0.018	0.011
MTV (continuous)		0.997	0.985–1.009	0.621		1.001	0.987–1.015	0.890	
TLG	Low vs. high	1.480	0.744–2.945	0.264	0.261	3.620	1.108–11.830	0.033	0.023
TLG (continuous)		1.000	0.998–1.001	0.583		1.000	0.998–1.002	0.944	
Pseudotime	Early vs. late	1.682	0.846–3.344	0.138	0.134	6.175	1.481–25.740	0.012	0.004
Pseudotime (continuous)		0.963	0.205–4.531	0.962		1.829	0.288–11.610	0.522	

**Table 2.** Univariate Cox regression analysis for survival. *HR* hazard ratio, *CI* confidence interval, *LRT* log-rank test.

Variable	Categories	MTV model		TLG model		Pseudotime model	
		HR (95% CI)	P-value	HR (95% CI)	P-value	HR (95% CI)	P-value
Age	< 66 vs. 66 ≤	2.371 (1.116–5.033)	0.025	2.427 (1.141–5.163)	0.021	2.413 (1.137–5.117)	0.022
Adjuvant chemotherapy	No vs. yes	0.177 (0.074–0.421)	< 0.001	0.174 (0.074–0.407)	< 0.001	0.166 (0.071–0.388)	< 0.001
Initial CEA	Low vs. high	2.786 (1.367–5.677)	0.005	2.727 (1.334–5.573)	0.006	2.721 (1.338–5.533)	0.006
Pathological T stage after CCRT	ypT0 vs. ypT1/is	0.691 (0.071–6.704)	0.750	0.731 (0.075–7.138)	0.788	0.655 (0.067–6.388)	0.875
	ypT0 vs. ypT2	0.522 (0.144–1.894)	0.323	0.583 (0.162–2.095)	0.409	0.481 (0.133–1.740)	0.301
	ypT0 vs. ypT3	0.581 (0.183–1.846)	0.358	0.650 (0.204–2.069)	0.466	0.541 (0.171–1.714)	0.384
	ypT0 vs. ypT4	0.524 (0.096–2.870)	0.456	0.478 (0.087–2.626)	0.396	0.382 (0.070–2.093)	0.558
Pathological N stage after CCRT	ypN0 vs. ypN1	4.298 (1.873–9.863)	< 0.001	4.528 (1.947–10.532)	< 0.001	4.334 (1.873–10.027)	< 0.001
	ypN0 vs. ypN2	10.204 (3.326–31.305)	< 0.001	11.239 (3.649–34.610)	< 0.001	10.250 (3.349–31.371)	< 0.001
MTV	Low vs. High	2.816 (0.968–8.194)	0.057				
TLG	Low vs. High			2.920 (0.781–8.718)	0.080		
Pseudotime	Early vs. Late					5.095 (1.187–21.874)	0.028

**Table 3.** Multivariate Cox regression analysis for overall survival. *HR* hazard ratio, *CI* confidence interval.

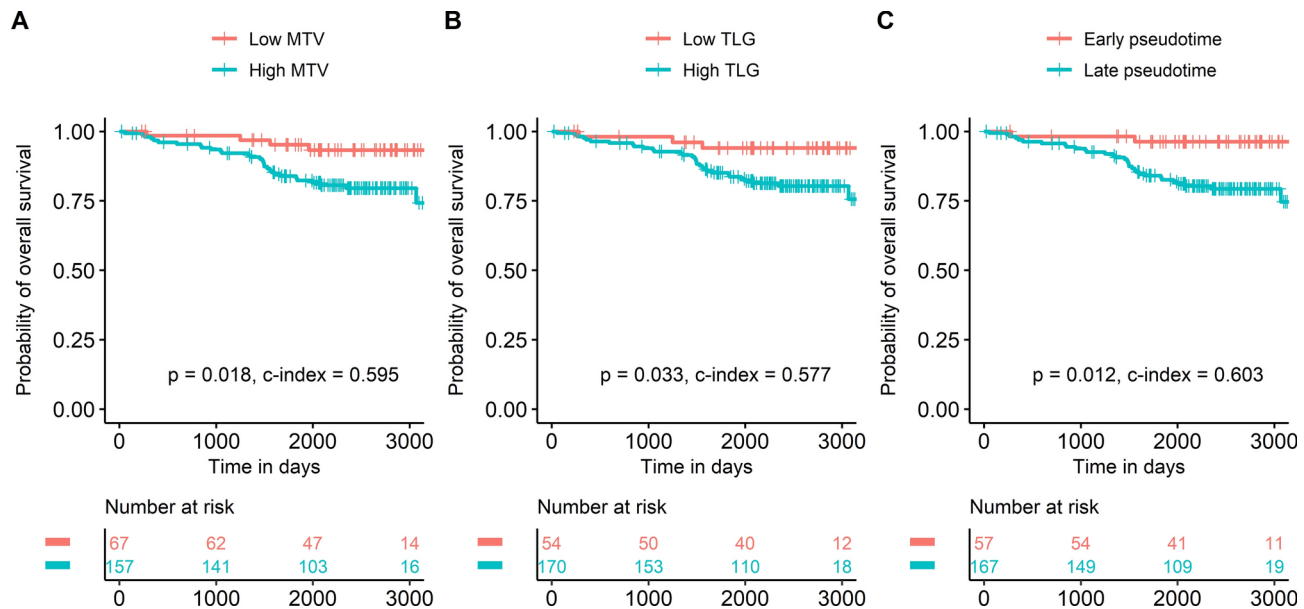


**Fig. 4.** Survival curves according to MTV, TLG, and pseudotime. MTV (A), TLG (B), and pseudotime (C) of the primary tumor were significant prognostic factors for overall survival.

## Data availability

The datasets used and analyzed during the current study are available from the corresponding author upon reasonable request.

Received: 28 July 2024; Accepted: 11 December 2024

Published online: 28 December 2024

## References

1. Delbeke, D. & Martin, W. H. PET and PET-CT for evaluation of colorectal carcinoma. *Semin. Nucl. Med.* **34**, 209–223 (2004).
2. Shin, S. S. et al. Preoperative staging of colorectal cancer: CT vs integrated FDG PET/CT. *Abdom. Imaging* **33**, 270–277 (2008).
3. Memon, S. et al. Systematic review of FDG-PET prediction of complete pathological response and survival in rectal cancer. *Ann. Surg. Oncol.* **21**, 3598–3607 (2014).
4. Calvo, F. A. et al. <sup>18</sup>F-FDG PET/CT-based treatment response evaluation in locally advanced rectal cancer: A prospective validation of long-term outcomes. *Eur. J. Nucl. Med. Mol. Imaging* **40**, 657–667 (2013).
5. Jo, H. J., Kim, S.-J., Lee, H. Y. & Kim, I. J. Prediction of survival and cancer recurrence using metabolic volumetric parameters measured by <sup>18</sup>F-FDG PET/CT in patients with surgically resected rectal cancer. *Clin. Nucl. Med.* **39**, 493–497 (2014).
6. Pyo, D. H. et al. A nomogram for predicting pathological complete response to neoadjuvant chemoradiotherapy using semiquantitative parameters derived from sequential PET/CT in locally advanced rectal cancer. *Front. Oncol.* **11**, 742728 (2021).
7. Ha, S., Choi, H., Paeng, J. C. & Cheon, G. J. Radiomics in oncological PET/CT: A methodological overview. *Nucl. Med. Mol. Imaging* **53**, 14–29 (2019).
8. Lovinsosse, P. et al. FDG PET/CT radiomics for predicting the outcome of locally advanced rectal cancer. *Eur. J. Nucl. Med. Mol. Imaging* **45**, 365–375 (2018).
9. Bundschuh, R. A. et al. Textural parameters of tumor heterogeneity in <sup>18</sup>F-FDG PET/CT for therapy response assessment and prognosis in patients with locally advanced rectal cancer. *J. Nucl. Med.* **55**, 891–897 (2014).
10. Lee, H. et al. Prognostic significance of pseudotime from texture parameters of FDG PET/CT in locally advanced non-small-cell lung cancer with tri-modality therapy. *Cancers* **14**, 3809 (2022).
11. Trapnell, C. Defining cell types and states with single-cell genomics. *Genome Res.* **25**, 1491–1498 (2015).
12. Xiang, R. et al. Identification of subtypes and a prognostic gene signature in colon cancer using cell differentiation trajectories. *Front. Cell Dev. Biol.* **9**, 705537 (2021).
13. Campbell, K. R. & Yau, C. Uncovering pseudotemporal trajectories with covariates from single cell and bulk expression data. *Nat. Commun.* **9**, 2442 (2018).
14. Orlhac, F. et al. Tumor texture analysis in <sup>18</sup>F-FDG PET: Relationships between texture parameters, histogram indices, standardized uptake values, metabolic volumes, and total lesion glycolysis. *J. Nucl. Med.* **55**, 414–422 (2014).
15. Hatt, M. et al. <sup>18</sup>F-FDG PET uptake characterization through texture analysis: Investigating the complementary nature of heterogeneity and functional tumor volume in a multi-cancer site patient cohort. *J. Nucl. Med.* **56**, 38–44 (2015).
16. Fang, Y.-H.D. et al. Development and evaluation of an open-source software package “CGITA” for quantifying tumor heterogeneity with molecular images. *Biomed. Res. Int.* **2014**, 248505 (2014).
17. Blei, D. M., Kucukelbir, A. & McAuliffe, J. D. Variational inference: A review for statisticians. *J. Am. Stat. Assoc.* **112**, 859–877 (2017).

## Acknowledgements

This work was supported by the National Research Foundation of Korea (NRF) grants funded by the Korean government (MSIT) (RS-2023-00239231, RS-2024-00334782), and the Future Medicine 20\*30 Project of the Samsung Medical Center (#SMO1240791).

### Author contributions

H Lee and JY Choi designed the study. H Lee analyzed and interpreted the data. H Lee was a major contributor to writing the manuscript. YB Cho, HC Kim, CH Park, and YS Park contributed to data curation. SH Hyun and JY Choi provided a critical revision of the article. All authors read and approved the final manuscript.

### Competing interests

The authors declare no competing interests.

### Additional information

**Supplementary Information** The online version contains supplementary material available at <https://doi.org/10.1038/s41598-024-83109-9>.

**Correspondence** and requests for materials should be addressed to J.Y.C.

**Reprints and permissions information** is available at [www.nature.com/reprints](http://www.nature.com/reprints).

**Publisher's note** Springer Nature remains neutral with regard to jurisdictional claims in published maps and institutional affiliations.

**Open Access** This article is licensed under a Creative Commons Attribution-NonCommercial-NoDerivatives 4.0 International License, which permits any non-commercial use, sharing, distribution and reproduction in any medium or format, as long as you give appropriate credit to the original author(s) and the source, provide a link to the Creative Commons licence, and indicate if you modified the licensed material. You do not have permission under this licence to share adapted material derived from this article or parts of it. The images or other third party material in this article are included in the article's Creative Commons licence, unless indicated otherwise in a credit line to the material. If material is not included in the article's Creative Commons licence and your intended use is not permitted by statutory regulation or exceeds the permitted use, you will need to obtain permission directly from the copyright holder. To view a copy of this licence, visit <http://creativecommons.org/licenses/by-nc-nd/4.0/>.

© The Author(s) 2024